RADIAL DEBLURRING WITH FFTS

Christopher B. Webster and Stanley J. Reeves

Electrical and Computer Engineering Department
Auburn University
Auburn, AL 36849
(334) 844-1835, 1821
{webstcb,reevesj}@auburn.edu

ABSTRACT

Radial blurring (sometimes called zoom blurring) of an image is a challenging problem because it is a shift-variant blur. As one travels outward from the center of an image, the blur length increases linearly with distance from the center. This shift-variant characteristic precludes the use of other traditional FFT-based deblurring techniques. We propose a way around this problem by transforming the coordinate system of the blurred image into one in which the blur is LSI. Equivalently, the blurred image is sampled in a particular nonuniform fashion so that the blur becomes LSI in the new discrete-space coordinates. As a result, the blur can be modeled by convolution so that FFT-based deblurring can be used.

Index Terms— radial blur, zoom blur

1. INTRODUCTION

While we have found no literature explicitly addressing radial blurring or deblurring, this blur can occur under certain conditions. Sometimes referred to as a zoom blur, a radial blur arises when a picture (or video) is taken as the imaging device is rapidly approaching the desired object. Such situations can occur with aerial photography as well as video-based missile systems. Figure 1 demonstrates the origin and mathematical model of the blur. The variable x represents the horizontal distance from the camera's location to the object in question, and v is the camera speed. The hollow rectangle is the object of interest, and p can be viewed as the vertical distance in the object plane seen by the camera. As time t increases and the camera approaches the object, p becomes smaller while the size of the object remains the same. This process creates a time-dependent scaling of the object in the camera image plane. This scale factor is represented by k. If the exposure time or speed is significant relative to the distance, the image will reflect a blurring of the object as it is progressively scaled and recorded by the camera. The result of this process is the integration (summation) of a sequence of continually scaled images as shown in Figure 2.

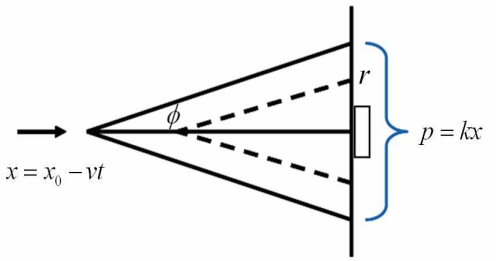

Fig. 1. Blur origin

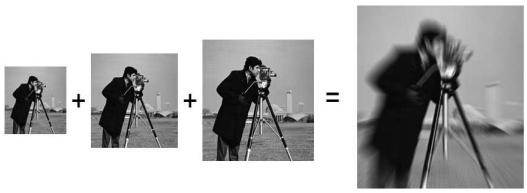

Fig. 2. Radial blurring

The major challenge with this type of blur is that the system is shift-variant. The blur is a type of motion blur. However, whereas typical motion blurring assumes that the object moves at a uniform rate during exposure, in this case the motion is different at each point in the object. In fact, the blur length increases linearly as one travels outward from the center of the image.

This fact renders traditional convolution-based deblurring methods unusable [1]. Iterative algorithms are generally necessary when the blur is not LSI [2], and these algorithms typically require a great deal more computation than closed-form algorithms based on the FFT. The inability to use FFTs in the deblurring process may be seriously problematic in the case of video-based guidance due to the need for real-time restored

images of the object being tracked. If the image can be resampled into a space in which the blur is a constant linear motion blur, then convolution—and hence FFTs—can be used to accomplish deblurring.

A related, well known idea—homomorphic filtering—has been studied by Oppenheim et al. in which they use a pointwise transformation on the dependent axis before and after convolution [3]. In the proposed case, the independent axis undergoes the transformation instead. That is, the spatial domain is warped so that an operation that was otherwise another type of integral becomes a convolution sandwiched between two geometric transformations.

We propose to transform the coordinate system of the blurred image into one in which the blur is LSI. Equivalently, the blurred image will be sampled in a particular nonuniform fashion so that the blur becomes LSI in the new discrete-space coordinates. As a result, the blur can be modeled by convolution so that we can perform closed-form FFT-based deblurring.

2. MATHEMATICAL DEVELOPMENT

The representative equation for the original blurred system is shown in (1) below, where g is the unblurred image, x is the horizontal spatial coordinate, r is the vertical spatial coordinate, and t represents time. The vertical spatial coordinate is actually a signed radius, assuming the object of interest is 2-dimensional. This introduces a θ term related to every position r, which expresses the angle of the coordinate system from the perspective of the observer relative to the horizon. Because the blur is one-dimensional for any given θ, the observation equation is expressed with a subscript θ for each y (and subsequently each g). ϕ is taken now to be the view angle of an arbitrary pixel whose linear distance from the center of the object is p.

$$y_\theta(\phi) = \int_0^{t_1} g_\theta(r(\phi, t))dt \tag{1}$$

From the diagram in Figure 1,

$$r = x\ \tan(\phi),\ \frac{dx}{dt} = -v \tag{2}$$

Through a change of variables, we obtain

$$y_\theta(\phi) = \frac{1}{v}\int_{x_0 - vt_1}^{x_0} g_\theta(x\ \tan(\phi))dx \tag{3}$$

In order to transform the blur to a convolution model, the spatial dimension must be changed so that scaling becomes a shift. In (4), (5), and (6), a change of variables is performed so that the limits of integration are now logarithmic terms and the integrand contains an exponential term. Let

$$z = \log(x) + \log(\tan(\phi)),\ \ e^z = x\ \tan(\phi) \tag{4}$$

Then

$$dz = \frac{1}{x}dx = \frac{\tan(\phi)}{e^z}dx \tag{5}$$

$$dx = \frac{1}{\tan(\phi)}e^z dz \tag{6}$$

Using these equations to do a change of variables on (3):

$$y_\theta(\phi) = \frac{1}{\tan(\phi)}\int_{\log(d_1)+\log(\tan(\phi))}^{\log(d_2)+\log(\tan(\phi))} e^z g(e^z)dz \tag{7}$$

where

$$d_1 = x_0 - vt_1,\ \ d_2 = x_0$$

In (7), the change of variables has been completed, but the integral is not obviously in convolution form. Define

$$h_\theta(z) = e^z g_\theta(e^z),\ \ \rho_i = \log(d_i),\ \ \alpha = \log(\tan(\phi)) \tag{8}$$

Using these expressions, we obtain:

$$\tilde{y}_\theta(\alpha) = \int_{\rho_1+\alpha}^{\rho_2+\alpha} h(z)dz \tag{9}$$

The we define

$$\tilde{y}_\theta(\alpha) = y_\theta(\log(\tan(\phi))) \tag{10}$$

For convenience, the limits on integration are expressed as multiplying the integrand by a pulse function in (11):

$$\tilde{y}_\theta(\alpha) = \int_{-\infty}^{\infty}[u(z-\alpha-\rho_1) - u(z-\alpha-\rho_2)]h_\theta(z)dz \tag{11}$$

We observe that this is equivalent to

$$\tilde{y}_\theta(\alpha) = [u(\alpha-\rho_1) - u(\alpha-\rho_2)] * h_\theta(\alpha) \tag{12}$$

Accordingly, (12) demonstrates that the forward model has been transformed into convolution with a uniform motion blur in a spatially transformed coordinate system.

3. EXPONENTIALLY SPACED SAMPLING

To express the blur operation in a discrete-space setting, the image must be radially sampled with an exponential spacing to achieve the desired shift-invariant result. By radial sampling, we mean along a line of pixels from one boundary of the image to the opposite boundary while passing through the center. These lines of pixels are taken at various angles, and then the lines of pixels are placed in columns to form a new rectangular image. Because these sample locations do not lie on a regular grid, an interpolation scheme must be used [4, 5]. A visualization of this sampling pattern is shown in Figure 3. The center of the image would be located at (0,0), and the square represents the boundaries of the image.

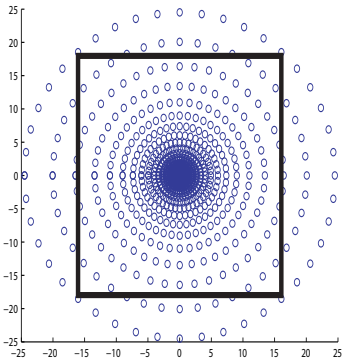

Fig. 3. Sampling Layout

Because the sampling is done radially, two parameters to consider are the quantity of sampling angles and the relative sample spacing. As the number of angles increases, the detail retained from the original image data increases. However, this also increases the computational time proportionately. The sampling must be dense enough to fully sample the image at the outer boundaries. In our experiments, we found that using 720 angles maintained the desired detail given the level of smoothing required to overcome noise behavior. Low-noise or high-resolution images would require more angles. The exponential spacing of the sampling pattern varies depending on the size of the input image. This spacing is dictated by the size of the input image; the spacing at the outer boundaries must be equivalent to the sampling of the blurred image to avoid aliasing.

4. BLUR MODELING

In order to test the functionality of the process, test images can be constructed via two different methods. The first method involves implementing the discretized blurring model on an unblurred image. The image is sampled radially, then blurred by column using FFTs. The image is then reconstructed in its original space using 2-D interpolation. This constitutes a radially blurred image that can then be used to test radial deblurring algorithms.

The second method forms the blurry image by using resizing and summation. The original image is taken and resized by uniform increments of the scale factor to be larger and larger, and all the resulting images are then added together. The process can be seen in Figure 2. This method is useful in that artifacts due to the radial sampling process can be avoided, and one can test the algorithm when the blurring and deblurring process are not structurally the same. Furthermore, different boundary conditions can be used as compared to the FFT-based radial blurring method.

5. DEBLURRING METHOD

The deblurring procedure begins with the radial sampling of the blurry image, as detailed in Section 3. To obtain the entire image in this process, the maximum radius of sampling must be equal to $\frac{\sqrt{2}}{2}N$, where N is the length of a side of the image. After stacking these radial samples into columns, the resulting image resembles Figure 4. The black arches at the bottom of the image result from sampling wide enough to obtain the corners of the original image. Because the sampling pattern is a circle, some of the sample points will fall outside the image frame. These undefined samples are supplied by replicating the last known good pixel value inside the image in that direction. The blur is now a one-dimensional motion blur at an angle of 90 degrees. The radial-space image is then deblurred (columnwise) via a simple FFT-based regularized restoration algorithm. For simplicity, the regularization operator was set to identity, and the regularization parameter was chosen by trial and error. The order of magnitude of the regularization parameter determined the characteristics of the result, and it was found that an order of 10^{-3} produced the sharpest results. Symmetric extension was used to extend the boundaries to reduce edge artifacts, although more complex but effective methods are available [6].

Once the deblurring is complete, the radial sampling is reversed—a 2-dimensional interpolation is performed to fill in the unknown pixels using a nonuniform interpolation algorithm based on Delaunay triangularization. This process (the 2-dimensional interpolation) is the main bottleneck in the procedure, requiring more than 90% of the total computation time. Fortunately, most of the computation can be done in advance to eliminate this bottleneck.

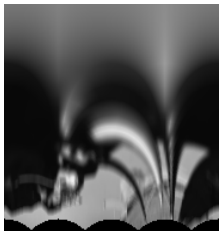

Fig. 4. Radial-space image

6. RESULTS

Figure 5 is the cameraman picture blurred with a 20% FFT-based radial blur and then reconstructed. The artifacts produced in the image mainly result from sharp edges around the boundary of the original image. These can be significantly

reduced if the outer border of the original image is free from highly detailed objects or if a more sophisticated boundary-compensation scheme is used.

Fig. 5. FFT-blurred image with reconstruction

Figure 6 is a picture of a fighter jet blurred (via the FFT method) with a severe 25% blur. This picture illustrates a rather extreme case for this method. Generally, blurs larger than this extend beyond the boundaries of the image, creating serious artifacts in the deblurring processing and therefore making adequate restorations very difficult.

Fig. 6. Severe 25% blur and reconstruction

The last set of pictures represents blurs created through the summation method with a blur of approximately 15%. Figure 7 shows the jet image blurred and then reconstructed. The image is recovered well from this method of blurring.

Fig. 7. Summation-blurred image with reconstruction

7. CONCLUSION

The proposed method performs well on images in which the main details are not blurred close to the image boundaries. During the restoration process, these sharp details produce noticeable ringing effects. These effects are evident in the restoration of the cameraman, which contains significant detail at the boundaries.

One of the interesting opportunities in this process is that any level of scaling (within the range of the scaled images that comprise the blurry image) can be recovered. To recover a particular scaling, one must simply define the shift of the pulse in the resampled domain so that the deconvolution process recovers the image with that particular shift; a given shift translates into a given "origin" in terms of the scaling of the image. In this way, the largest of the scaled copies of the image can be recovered to obtain maximum resolution.

A number of issues remain to be worked out. First, the effects of noise have not been considered in this work. Noise effects will be more significant at further distances from the radial center. Shift-invariant smoothing in the resampled domain may not yield the best possible tradeoff between noise suppression and noise amplification. Second, the best approach to handling boundaries must be investigated. Third, we must study the tradeoffs involved in sampling density versus restoration quality. However, the present work provides a proof of concept for a highly efficient approach to deblurring radially blurred images.

8. REFERENCES

[1] H. C. Andrews and B. R. Hunt, *Digital Image Restoration*, Prentice-Hall, New Jersey, 1977.

[2] Al Bovik, Ed., *Handbook of Video and Image Processing*, chapter Iterative Image Restoration, pp. 235–252, Academic Press, Maine, second edition, 2005.

[3] A. V. Oppenheim, R. W. Schafer, and T. G. Stockham, Jr., "Nonlinear filtering of multiplied and convolved signals," *Proceedings of the IEEE*, vol. 56, no. 8, pp. 1264–1291, August 1968.

[4] H. H. Hou and H. C. Andrews, "Cubic splines for image interpolation and digital filtering," *ASSP*, vol. ASSP-26, pp. 508–517, 1978.

[5] M. Unser, A. Aldroubi, and M. Eden, "Fast b-spline transforms for continuous image representation and interpolation," *PAMI*, vol. PAMI-13, pp. 277–285, 1991.

[6] S. J. Reeves, "Fast image restoration without boundary artifacts," *IEEE Transactions on Image Processing*, vol. 14-10, pp. 1448–1453, 2005.